

Reversible Two-Electron Redox Reactions Involving Tetralithio/Dilithio Palladole, Platinacycle, and Dicupra[10]annulene

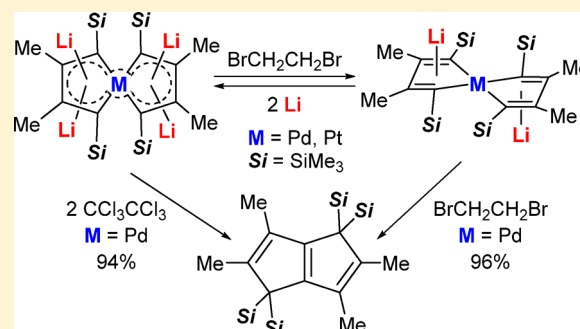
Zhe Huang,[†] Yongliang Zhang,[†] Wen-Xiong Zhang,^{*,†} and Zhenfeng Xi^{*,†,‡}

[†]Beijing National Laboratory for Molecular Sciences (BNLMS), Key Laboratory of Bioorganic Chemistry and Molecular Engineering of Ministry of Education, College of Chemistry, Peking University, Beijing 100871, China

[‡]State Key Laboratory of Organometallic Chemistry, Shanghai Institute of Organic Chemistry (SIOC), Shanghai 200032, China

Supporting Information

ABSTRACT: The reaction chemistry of metalla-aromatics is fundamentally interesting. In this work, we find that tetralithio spiroaromatic palladole and platinacycle complexes **1** undergo selective two-electron oxidation with 1,2-dibromoethane as a mild oxidant, affording their corresponding dilithio spiro metallacyclopentadienes **3**. These dilithio spiro complexes **3** can be reductively transformed to their corresponding tetralithio spiroaromatic complexes **1** with metallic lithium. When treated with an appropriate amount of oxidants, both **1** and **3** can generate 1,4-dihydropentalene derivatives **5** via a mechanism involving reductive elimination and silyl migration, as supported by density functional theory calculation. Similarly, tetralithio aromatic dicupra[10]annulene **2** can also undergo the reversible two-electron redox reaction mentioned above. These results improve our understanding of the reactivity of metalla-aromatic compounds.



INTRODUCTION

The chemistry of metalla-aromatics is a fascinating topic, because such compounds with metal(s) in the aromatic system may show novel reactivity that is not seen for classical organic aromatic compounds.¹ Recently, we have found that 1,4-dilithio-1,3-butadienes² could be viewed as non-innocent ligands, using their LUMO (π^* orbital) to accept d electrons of transition metals. Consequently, the reaction of 1,4-dilithio-1,3-butadienes with low-valent transition metal complexes generated a number of novel metalloaromatic compounds,³ such as tetralithio spiro metalla-aromatics [**1** (Scheme 1)]^{3d} and tetralithio aromatic dicupra[10]annulenes [**2** (Scheme 1)].^{3c} The electronic structures and bonding modes of these tetralithio metalla-aromatics have been theoretically studied.⁴ However, their reaction chemistry has not been investigated.

As for dilithio aromatic main-group metalloles, an interesting reversible redox process between **I/I'** and **II/II'** has been reported (Scheme 1a).⁵ Because our metalla-aromatic compounds **1** and **2** are very much different from **I** and **II** in terms of structures, bonding modes, and metals, we expected that they should have different redox reactivity.

RESULTS AND DISCUSSION

First, we carried out the oxidation of spiro metalla-aromatics **1a** and **1b** using 1,2-dibromoethane as a mild oxidant (Scheme 2). By slowly adding dibromoethane to the solution of **1a** while stirring, we obtained dilithio spiro palladole **3a** in 99% isolated yield. Ethylene was observed as the reduction product by *in situ* nuclear magnetic resonance (NMR) (see the Supporting

Information), indicating a two-electron redox process. Each of the two lithium atoms in **3a** is coordinated by a tetrahydrofuran (THF) molecule, as judged from the ¹H NMR spectrum. Meanwhile, the reaction of **3a** with metallic lithium regenerated **1a** quantitatively, which revealed a reversible two-electron redox behavior between **1a** and **3a**. A similar redox process was found between spiroaromatic platinacycle **1b** and dilithio spiro platinacycle **3b**. Recently, we have found that the Li cations play an important role in the aromaticity of dilithio metalloles as they help to increase the extent of orbital overlap between the transition metal's d orbitals and the butadienyl π^* orbitals.^{3e} The formation of LiBr might be a driving force for this dearomatization process. To further investigate their redox behavior, a cyclic voltammetry experiment was attempted in a glovebox. However, **1a** and **1b** decomposed quickly in the electrolyte solution (THF/NBu₄PF₆ or THF/LiNTf₂) and no signal was observed.

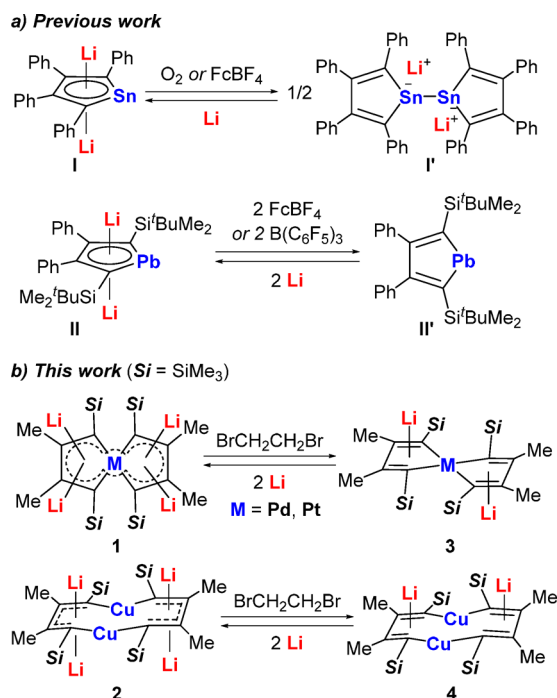
After the addition of 1,2-dimethoxyethane (DME) and recrystallization in hexane, single crystals of **3a-2DME** and **3b-2DME** were obtained (see the Supporting Information). As they have similar structures, here we discuss the structure of **3a** as an example. As shown in Figure 1, the structure of **3a** contains two metalloles sharing the Pd atom with a dihedral angle of 43.0°, which is slightly smaller than that in **1a** (50.2°).^{3d} The two lithium atoms are on the opposite sides of the metalloles and coordinated in η^5 mode. In contrast to the

Received: May 15, 2019

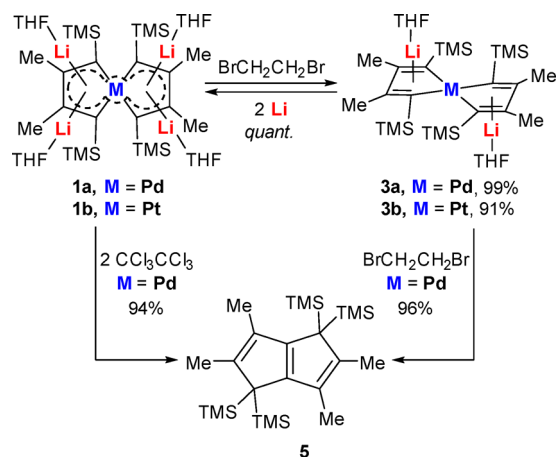
Published: July 9, 2019



Scheme 1. Reversible Redox Processes Involving Metalla-Aromatics from (a) Previous Work on Redox Processes Involving Dilithiostannole and Dilithioplumbole and (b) This Work on Redox Processes Involving Tetralithio Spiro Metalla-Aromatics and Dicupra[10]annulene



Scheme 2. Redox Process Involving Spiroaromatic Palladole/Platinacycle



aromatic structure of **1a**, the metallole moieties in **3a** exhibit nonplanar structures with C–C bond alternation. For example, the C1–C2, C2–C3, and C3–C4 bond lengths are 1.369(3), 1.490(3), and 1.368(3) Å, respectively, and the dihedral angle between the C1–C2–C3–C4 plane and the C1–C4–Pd1 plane is 10.1°. The Pd–Li bonds in **3a** (average of 2.634 Å) and Pt–Li bonds in **3b** (average of 2.650 Å) are also longer than those in **1a** (average of 2.522 Å) and **1b** (average of 2.555 Å). In addition, the resonance signals in the ⁷Li NMR spectra were observed at –1.52 ppm for **3a** and –3.51 ppm for **3b**, which are shifted downfield compared to those of **1a** (–5.14 ppm) and **1b** (–6.34 ppm),^{3d} indicating a weakened shielding effect. These structural and spectroscopic features suggest that

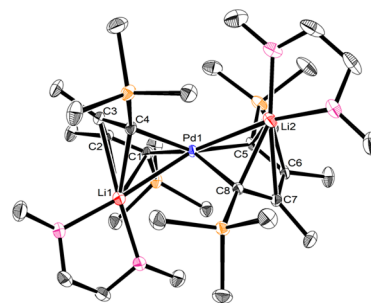


Figure 1. ORTEP drawing of **3a-2DME** with 30% thermal ellipsoids. Hydrogen atoms have been omitted for the sake of clarity. Selected bond lengths or distances (angstroms): Pd1–C1, 2.122(2); Pd1–C4, 2.151(2); Pd1–C5, 2.096(2); Pd1–C8, 2.162(2); C1–C2, 1.369(3); C2–C3, 1.490(3); C3–C4, 1.368(3); C5–C6, 1.364(3); C6–C7, 1.489(3); C7–C8, 1.375(3); Li1–C1, 2.368(5); Li1–C2, 2.398(5); Li1–C3, 2.434(5); Li1–C4, 2.245(5); Li2–C5, 2.376(5); Li2–C6, 2.387(5); Li2–C7, 2.374(5); Li2–C8, 2.166(5).

3a and **3b** are best described as ate complexes formed by a spiro metallole dianion and two lithium cations.

When **3a** was further treated with 1.0 equiv of dibromoethane in THF at room temperature, an insoluble black solid precipitated immediately, affording product **5** in 96% isolated yield (Scheme 2). The X-ray photoelectron spectroscopy (XPS) experiment suggested that the insoluble black solid contained Pd(0), as the Pd 3d_{5/2} peak was observed at 335.69 eV.⁶ Product **5** could also be obtained in 94% yield directly from the oxidation of **1a** using 2.0 equiv of hexachloroethane as the oxidant, and 1,1,2,2-tetrachloroethylene was found as the reduction product by *in situ* NMR.

The molecular structure of **5** was confirmed by X-ray diffraction analysis. As shown in Figure 2, the two fused five-

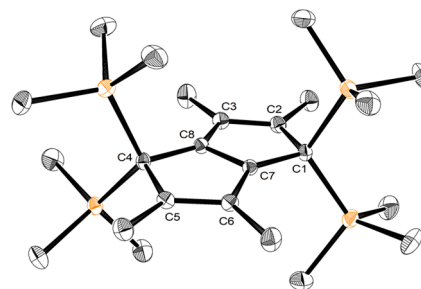


Figure 2. ORTEP drawing of **5** with 30% thermal ellipsoids. Hydrogen atoms have been omitted for the sake of clarity. Selected bond lengths or distances (angstroms): C1–C2, 1.5211(17); C1–C7, 1.5060(17); C2–C3, 1.3648(18); C3–C8, 1.4510(17); C4–C5, 1.5213(16); C4–C8, 1.5084(17); C5–C6, 1.3640(18); C6–C7, 1.4493(17); C7–C8, 1.3762(17).

membered rings are coplanar with three double bonds C2=C3, C5=C6, and C7=C8, indicating a 1,4-dihydropentalene structure. Such tetrakis(trimethylsilyl)-1,4-dihydropentalene derivatives are structurally interesting compounds but difficult to access with known synthetic methods.⁷

To gain further understanding of the reaction mechanism, density functional theory (DFT) calculation was carried out (see the Supporting Information), and the calculated potential energy surfaces are shown in Figure 3. The two-electron oxidation of **3a** could afford spiro palladole **Int-1**, which then undergoes reductive elimination to form a nine-membered palladacycle with one double bond coordinated to the Pd atom

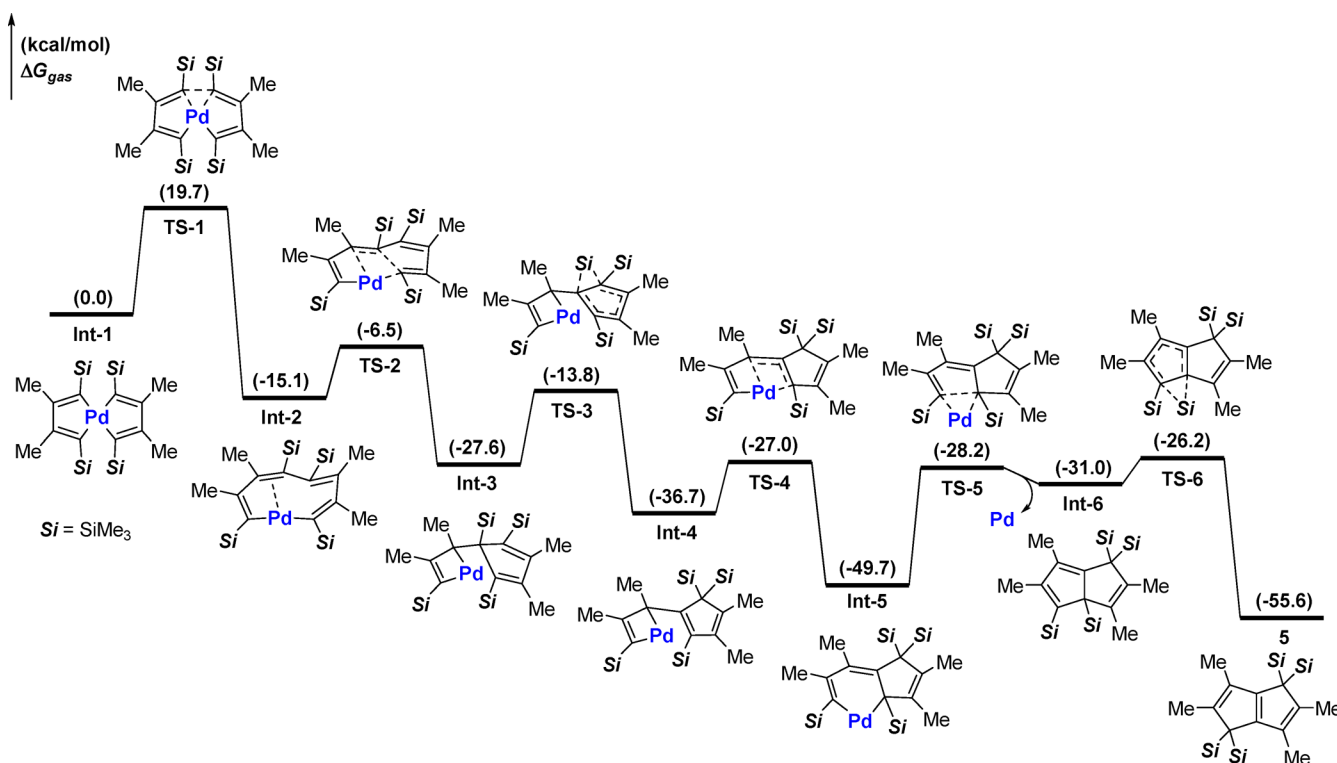
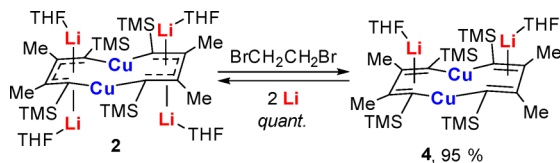


Figure 3. Density functional theory-calculated potential energy surfaces for the formation of **5**.

(**Int-2**). The 1,2-insertion of the double bond results in the formation of the first five-membered ring (**Int-3**). Subsequent 1,5-silyl migration followed by insertion of the double bond in the five-membered ring to the C–Pd bond in the palladacycle gives **Int-5** with a six-membered palladacycle. Then, the second reductive elimination generates **Int-6** with the release of Pd(0), and the second 1,5-silyl migration affords the final product **5**. The second reductive elimination (from **Int-5** to **Int-6**) is the rate-determining step with an energy barrier of 21.5 kcal/mol, which suggests that this pathway is feasible at room temperature.

Inspired by these results, we moved to the oxidation of tetralithio aromatic dicupra[10]annulene **2**, another metalla-aromatic complex with an interesting structure (Scheme 3), as

Scheme 3. Redox Process Involving Dicupra[10]annulene



the theoretical study has also revealed the importance of Li in its aromaticity.^{4b} Similarly, **2** could also undergo a two-electron oxidation process to afford dilithio dicupra[10]annulene **4** in 95% yield by treatment with 1.0 equiv of dibromoethane in THF. The reduction of **4** with metallic lithium regenerated **2** quantitatively. In other words, there is a reversible two-electron redox process between **2** and **4**, as well. The molecular structure of **4**·2DME was also confirmed by X-ray crystallographic analysis (Figure 4). It should be mentioned that in our previous work, another dilithio dicupra[10]annulene with different substituents has been obtained and proposed as the

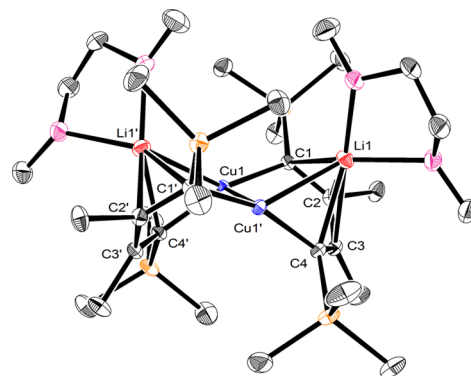


Figure 4. ORTEP drawing of **4**·2DME with 30% thermal ellipsoids. Hydrogen atoms have been omitted for the sake of clarity. Selected bond lengths or distances (angstroms): Cu1–Cu1', 2.4297(3); Cu1–C1, 1.9379(11); Cu1'–C4, 1.9555(11); C1–C2, 1.3574(16); C2–C3, 1.5252(16); C3–C4, 1.3632(16); Li1–C1, 2.409(2); Li1–C2, 2.239(2); Li1–C3, 2.405(2); Li1–C4, 2.235(2).

key intermediate in the synthesis of the tetralithio dicupra[10]annulene.^{3c}

CONCLUSIONS

In summary, we describe a reversible two-electron redox process between tetralithio spiroaromatic palladole/platinacycle **1** and dilithio spiro palladole/platinacycle **3** as well as tetralithio aromatic dicupra[10]annulene **2** and dilithio dicupra[10]annulene **4**. These results improved our understanding of reactivity of metalla-aromatic compounds. With these oxidation reactions, multisubstituted 1,4-dihydropentadiene derivative **5** with an interesting structure was obtained.

EXPERIMENTAL SECTION

General Procedures. Unless otherwise noted, all starting materials were commercially available and were used without further purification. **1a** and **1b** were prepared by our reported method.^{3d} Solvents were purified with an MBraun SPS-800 Solvent Purification System. All reactions were carried out under a dry and oxygen-free argon atmosphere under a slight positive pressure by using Schlenk techniques or under an argon atmosphere in a Vigor (SG1200/750TS-F) glovebox. The argon in the glovebox was constantly circulated through a copper/molecular sieve catalyst unit. The oxygen and moisture concentrations in the glovebox atmosphere were monitored by an O₂/H₂O Combi-Analyzer to ensure both were always below 1 ppm.

Analytical Techniques. ¹H and ¹³C NMR spectra were recorded on a Bruker ARX400 spectrometer (FT, 400 MHz for ¹H; 100 MHz for ¹³C) or a Bruker AVANCE III spectrometer (FT, 500 MHz for ¹H; 126 MHz for ¹³C; 195 MHz for ⁷Li) at room temperature. High-resolution mass spectra (HRMS) were recorded on a Bruker Apex IV FTMS mass spectrometer using an ESI (electrospray ionization) source. XPS was carried out on an Axis Ultra imaging photoelectron spectrometer.

The single crystals of **3a-2DME**, **3b-2DME**, **4-2DME**, and **5** suitable for X-ray analysis were grown as shown in the [Experimental Section](#). Data collection was performed at 180 K on SuperNova diffractometer, using monochromated Mo K α radiation ($\lambda = 0.71073$ Å). Using Olex2, the structures were determined with the Superflip structure solution program using Charge Flipping or the ShelXS-97 structure solution program using direct methods and refined with the ShelXL refinement package using least squares minimization. Refinement was performed on *F*² anisotropically for all the non-hydrogen atoms by the full-matrix least-squares method. The hydrogen atoms were placed at the calculated positions and were included in the structure calculation without further refinement of the parameters. Crystal data, data collection parameters, and processing parameters are summarized in [Tables S1–S4](#). Crystallographic data have been deposited with the Cambridge Crystallographic Data Centre as supplementary publication nos. CCDC 1903991 (**3a-2DME**), CCDC 1903992 (**3b-2DME**), CCDC 1904049 (**4-2DME**), and CCDC 1903990 (**5**). Copies of these data can be obtained free of charge from the Cambridge Crystallographic Data Centre via www.ccdc.cam.ac.uk/data_request/cif. The thermal ellipsoid plots in the figures were drawn with Ortep-3 version 1.08.

Synthesis of Dicupra[10]annulene 2. Complex **2** was synthesized by a modified method based on our reported one.^{3c} Dilithio reagent (178.8 mg, 0.75 mmol) was dissolved in hexane (6 mL) and added to the mixture of CuBr·SMe₂ (102.8 mg, 0.5 mmol) and metallic lithium (69 mg, 10 mmol) in Et₂O (6 mL). After the mixture had been stirred for 5 min, THF (2 mL) was added, and the mixture was stirred at room temperature for 12 h. The volatile substances were removed in vacuum, and the solid insoluble in hexane was removed by filtration. After removal of the solvent and recrystallization in hexane, **2** was obtained as dark red crystals in 83% yield (185.1 mg), which is much higher than that of the previous method.^{3c}

Oxidation of 1a, 1b, and 2 by 1,2-Dibromoethane. A THF solution of 1,2-dibromoethane (2 mL, 0.025 mol/L, 0.05 mmol) was added drop by drop to a THF solution of **1a** (43.6 mg, 0.05 mmol) at room temperature while being stirred. After the mixture had been stirred at room temperature for 15 min, the volatile substances were removed in vacuum and the white solid insoluble in hexane was removed by filtration. After removal of the solvent, **3a** was obtained as a dark yellow solid in 99% yield. Similarly, **3b** and **4** were obtained. After the addition of 1,2-dimethoxyethane (9.0 mg, 0.1 mmol) and recrystallization in hexane at –20 °C, single crystals of **3a-2DME**, **3b-2DME**, and **4-2DME** suitable for X-ray diffraction were obtained.

3a: dark yellow solid; isolated yield 99% (35.2 mg); ¹H NMR (500 MHz, C₆D₆, 25 °C) δ 0.51 (s, 36H, CH₃), 1.15 (m, 8H, CH₂), 2.17 (s, 12H, CH₃), 3.30 (m, 8H, CH₂); ¹³C NMR (126 MHz, C₆D₆, 25 °C) δ 3.94 (12 CH₃), 23.96 (4 CH₃), 25.21 (4 CH₂), 68.96 (4 CH₂),

162.44 (4 quat. C), 188.76 (4 quat. C); ⁷Li NMR (195 MHz, THF-*d*₈, 25 °C) δ –1.52.

3b: green solid; isolated yield 91% (36.5 mg); ¹H NMR (500 MHz, C₆D₆, 25 °C) δ 0.50 (s, 36H, CH₃), 1.15 (m, 8H, CH₂), 2.20 (s, 12H, CH₃), 3.31 (m, 8H, CH₂); ¹³C NMR (126 MHz, C₆D₆, 25 °C) δ 3.85 (12 CH₃), 23.74 (4 CH₃), 25.21 (4 CH₂), 68.97 (4 CH₂), 160.66 (4 quat. C), 175.56 (4 quat. C); ⁷Li NMR (195 MHz, THF-*d*₈, 25 °C) δ –3.51.

4: pink solid; isolated yield 95% (34.8 mg); ¹H NMR (500 MHz, C₆D₆, 25 °C) δ 0.47 (s, 36H, CH₃), 1.20 (m, 8H, CH₂), 2.32 (s, 12H, CH₃), 3.40 (m, 8H, CH₂); ¹³C NMR (126 MHz, C₆D₆, 25 °C) δ 3.98 (12 CH₃), 25.25 (4 CH₂), 26.44 (4 CH₃), 69.21 (4 CH₂), 161.94 (4 quat. C); ⁷Li NMR (195 MHz, THF-*d*₈, 25 °C) δ –0.73.

Reduction of 3a, 3b, and 4 by Metallic Lithium. Metallic lithium (6.9 mg, 1.0 mmol) was added to the THF-*d*₈ solution of **3a** (35.7 mg, 0.05 mmol) in a NMR tube. The reaction was monitored by NMR, and after 12 h, **3a** was converted into **1a** quantitatively. Similarly, **3b** and **4** could be converted into **1b** and **2** quantitatively.

Oxidation of 2a by 1,2-Dibromoethane. A THF solution of 1,2-dibromoethane (2 mL, 0.025 mol/L, 0.05 mmol) was added drop by drop to a THF solution of **2a** (35.7 mg, 0.05 mmol) at room temperature while the solution was being stirred. After the mixture had been stirred at room temperature for 15 min, the volatile substances were removed in vacuum and the solid insoluble in hexane was removed by filtration. After the solvent had been removed, **5** was obtained in 96% yield (21.5 mg). Single crystals of **5** suitable for X-ray diffraction were obtained by recrystallization in hexane at –20 °C.

5: yellow solid; isolated yield 96% (21.5 mg); ¹H NMR (400 MHz, C₆D₆, 25 °C) δ 0.10 (s, 36H, CH₃), 2.05 (s, 6H, CH₃), 2.08 (s, 6H, CH₃); ¹³C NMR (100 MHz, C₆D₆, 25 °C) δ 1.55 (12 CH₃), 14.79 (2 CH₃), 16.93 (2 CH₃), 47.90 (2 quat. C), 131.50 (2 quat. C), 138.12 (2 quat. C), 153.05 (2 quat. C); HRMS *m/z* calcd for C₂₄H₄₈Si₄ 448.2828, found 448.2828.

Oxidation of 1a by Hexachloroethane. Hexachloroethane (23.7 mg, 0.10 mmol) was dissolved in THF (1 mL) and added drop by drop to the THF (4 mL) solution of **1a** (43.6 mg, 0.05 mmol) while the solution was being stirred. After the mixture had been stirred at room temperature for 15 min, the volatile substances were removed in vacuum and the solid insoluble in hexane was removed by filtration. After the solvent had been removed, **5** was obtained in 94% yield (21.0 mg).

In Situ NMR Studies. 1,2-Dibromoethane (18.8 mg, 0.1 mmol) was added to the THF-*d*₈ solution of **1a** (43.6 mg, 0.05 mmol) in a NMR tube. After 5 min, the NMR experiment was carried out and ethylene was observed as the reduction product (5.36 ppm in ¹H NMR and 123.36 ppm in ¹³C NMR). When hexachloroethane was used instead of 1,2-dibromoethane, tetrachloroethene was observed as the reduction product (121.32 ppm in ¹³C NMR).

DFT Calculations. All calculations were carried out with the GAUSSIAN 16 program package. The optimization structure and correction energy of all the minima and transition states were fully calculated at the B3LYP-D3 level using the LANL2DZ basis set (for Pd) and the 6-311G(d,p) basis set (for other elements) in the gas phase. Harmonic frequency calculations were performed at the same level for every structure to confirm it as a local minimum or transition state and to derive the thermochemical corrections for enthalpies and free energies. The intrinsic reaction coordinate (IRC) analysis was carried out throughout the pathways to confirm that all stationary points are smoothly connected to each other. See the [Supporting Information](#) for the calculation details and the full reference of Gaussian 16.

ASSOCIATED CONTENT

Supporting Information

The Supporting Information is available free of charge on the ACS Publications website at DOI: [10.1021/acs.organo.9b00295](https://doi.org/10.1021/acs.organo.9b00295).

Experimental and computational details, XPS spectrum, NMR data, and spectra for all new compounds (PDF)

Optimized Cartesian coordinates of all stationary points (XYZ)

Accession Codes

CCDC 1903990–1903992 and 1904049 contain the supplementary crystallographic data for this paper. These data can be obtained free of charge via www.ccdc.cam.ac.uk/data_request/cif, or by emailing data_request@ccdc.cam.ac.uk, or by contacting The Cambridge Crystallographic Data Centre, 12 Union Road, Cambridge CB2 1EZ, UK; fax: +44 1223 336033.

AUTHOR INFORMATION

Corresponding Authors

*E-mail: wx_zhang@pku.edu.cn.

*E-mail: zfxi@pku.edu.cn.

ORCID

Zhe Huang: 0000-0002-9201-9491

Yongliang Zhang: 0000-0002-6671-2495

Wen-Xiong Zhang: 0000-0003-0744-2832

Zhenfeng Xi: 0000-0003-1124-5380

Notes

The authors declare no competing financial interest.

ACKNOWLEDGMENTS

This work was supported by the National Natural Science Foundation of China (21690061, 21725201, and 21572005) and the High-performance Computing Platform of Peking University.

REFERENCES

- (1) For selected reviews, see: (a) Cao, X.-Y.; Zhao, Q.; Lin, Z.; Xia, H. The Chemistry of Aromatic Osmacycles. *Acc. Chem. Res.* **2014**, *47*, 341–354. (b) Saito, M. Transition-Metal Complexes Featuring Dianionic Heavy Group 14 Element Aromatic Ligands. *Acc. Chem. Res.* **2018**, *51*, 160–169. (c) Zhu, C.; Xia, H. Carbolong Chemistry: A Story of Carbon Chain Ligands and Transition Metals. *Acc. Chem. Res.* **2018**, *51*, 1691–1700. (d) Wei, J.; Zhang, W.-X.; Xi, Z. The aromatic dianion metalloles. *Chem. Sci.* **2018**, *9*, 560–568. (e) Hua, Y.; Zhang, H.; Xia, H. Aromaticity: History and Development. *Youji Huaxue* **2018**, *38*, 11–28. (f) Wang, H.; Zhou, X.; Xia, H. Metallaaromatics Containing Main-group Heteroatoms. *Chin. J. Chem.* **2018**, *36*, 93–105. (g) Frogley, B. J.; Wright, L. J. Recent Advances in Metallaaromatic Chemistry. *Chem. - Eur. J.* **2018**, *24*, 2025–2038.
- (2) (a) Xi, Z. 1,4-Dilithio-1,3-dienes: Reaction and Synthetic Applications. *Acc. Chem. Res.* **2010**, *43*, 1342–1351. (b) Zhang, W.-X.; Xi, Z. Organometallic intermediate-based organic synthesis: organo-di-lithio reagents and beyond. *Org. Chem. Front.* **2014**, *1*, 1132–1139.
- (3) (a) Wei, J.; Zhang, W.-X.; Xi, Z. Dianions as Formal Oxidants: Synthesis and Characterization of Aromatic Dilithionickeloles from 1,4-Dilithio-1,3-butadienes and [Ni(cod)₂]. *Angew. Chem., Int. Ed.* **2015**, *54*, 5999–6002. (b) Wei, J.; Zhang, Y.; Zhang, W.-X.; Xi, Z. 1,3-Butadienyl Dianions as Non-Innocent Ligands: Synthesis and Characterization of Aromatic Dilithio Rhodacycles. *Angew. Chem., Int. Ed.* **2015**, *54*, 9986–9990. (c) Wei, J.; Zhang, Y.; Chi, Y.; Liu, L.; Zhang, W.-X.; Xi, Z. Aromatic Dicu[10]annulenes. *J. Am. Chem. Soc.* **2016**, *138*, 60–63. (d) Zhang, Y.; Wei, J.; Chi, Y.; Zhang, X.; Zhang, W.-X.; Xi, Z. Spiro Metalla-aromatics of Pd, Pt, and Rh: Synthesis and Characterization. *J. Am. Chem. Soc.* **2017**, *139*, 5039–5042. (e) Zhang, Y.; Wei, J.; Zhu, M.; Chi, Y.; Zhang, W.-X.; Ye, S.; Xi, Z. Tetralithio Metalla-aromatics with Two Independent Perpendicular Dilithio Aromatic Rings Spiro-fused by One Manganese Atom. *Angew. Chem., Int. Ed.* **2019**, *58*, 9625–9631.
- (4) (a) Grande-Aztatzi, R.; Mercero, J. M.; Matito, E.; Frenking, G.; Ugalde, J. M. The aromaticity of dicu[10]annulenes. *Phys. Chem. Chem. Phys.* **2017**, *19*, 9669–9675. (b) An, K.; Shen, T.; Zhu, J. Craig-Type Möbius Aromaticity and Antiaromaticity in Dimetalla[10]-annulenes: A Metal-Induced Yin-and-Yang Pair. *Organometallics* **2017**, *36*, 3199–3204. (c) Dimitrova, M.; Sundholm, D. The aromatic character of [10]annulenes and dicu[10]annulenes from current density calculations. *Phys. Chem. Chem. Phys.* **2018**, *20*, 1337–1346. (d) Liu, N.; Wang, J. Theoretical Studies on Aromaticity of Spiro Metallaaromatics of (C₁₀H₁₀M)²⁺ (M = Ni, Pd, Pt). *Chem. Res. Chin. Univ.* **2018**, *34*, 470–474.

(5) (a) Haga, R.; Saito, M.; Yoshioka, M. Reversible Redox Behavior between Stannole Dianion and Bistannole-1,2-Dianion. *J. Am. Chem. Soc.* **2006**, *128*, 4934–4935. (b) Haga, R.; Saito, M.; Yoshioka, M. Stepwise Oxidation of the Stannole Dianion. *Chem. - Eur. J.* **2008**, *14*, 4068–4073. (c) Saito, M.; Kuwabara, T.; Kambayashi, C.; Yoshioka, M.; Ishimura, K.; Nagase, S. Synthesis, Structure, and Reaction of Tetraethyldilithiostannole. *Chem. Lett.* **2010**, *39*, 700–701. (d) Saito, M.; Nakada, M.; Kuwabara, T.; Minoura, M. A reversible two-electron redox system involving a divalent lead species. *Chem. Commun.* **2015**, *51*, 4674–4676.

(6) Wagner, C. D.; Riggs, W. M.; Davis, L. E.; Moulder, J. F. *Handbook of X-Ray Photoelectron Spectroscopy*; Perkin-Elmer: Ramsey, MN, 2000.

(7) Cloke, F. G. N.; Kuchta, M. C.; Harker, R. M.; Hitchcock, P. B.; Parry, J. S. Trialkylsilyl-Substituted Pentalene Ligands. *Organometallics* **2000**, *19*, 5795–5798.